Nonconventional Pressure-Assisted Powder Consolidation Methods

J.R. Groza

Nonconventional consolidation methods have been developed to minimize the microstructural changes during compaction of metastable powder materials. The methods presented in this article combine short-time high-temperature exposure with either high-pressure application or plasma discharge. The current understanding of pressure sintering was used to identify the densification mechanisms for each process. When high pressure is applied, the contribution of plastic yielding to densification is augmented such that lower temperatures and shorter times than in conventional processes are conceivable for the overall compaction process. Plasma discharge results in particle surface activation that enhances particle sinterability and reduces high-temperature exposure. To illustrate the specifics of these new nonconventional consolidation methods, examples of short-time densification of difficult-to-sinter materials are presented.

Keywords
compaction, consolidation, densification, plasma, powder, pressure-assisted, sinterability

1. Introduction

NOVEL materials that combine unusual properties such as superplasticity in normally brittle materials, ferromagnetic properties in nonferromagnetic materials, or electronic materials with controlled band gaps have received considerable attention in recent years. Most of these materials are in powder form and attribute their unique properties to a metastable condition, e.g., amorphous, nanocrystalline, or nonequilibrium phase structures. As identified at a recent workshop, consolidation of these metastable powders is a major challenge, because they undergo phase transformations under high-temperature exposure.[1] Pressure application is known to assist the densification process by enhancing sintering processes and thus reducing the high-temperature exposure of the consolidating powders. Among the pressure-assisted compaction methods, hot isostatic pressing (HIP) has been well developed to produce fully dense microstructures under simultaneous application of pressure and temperature with minimal additions of sintering aids. However, the typical thermal exposure during HIP is around two thirds of the material melting point for a time on the order of hours. In the context of preserving the metastable structures, this high-temperature exposure almost always causes significant microstructural changes. Therefore, further reducing the high-temperature excursion of densifying materials has been a major goal for developing new consolidation processes. All these new processes combine higher pressures with lower temperatures and shorter times than HIP and are aimed at preserving the unique microstructures and properties of metastable materials.

The focus of the present article is on nonconventional pressure-assisted powder consolidation methods that are capable of minimizing the thermal exposure of highly metastable materials. Some of these methods combine an additional plasma activation component to powder consolidation. In particular, the current understanding of the pressure sintering process has been used to identify the mechanisms by which these nonconventional processing methods lead to powder compaction. Specific examples include Ceracon™, rapid omnidirectional consolidation (ROC), and plasma-activated sintering (PAS) methods. They are compared to more conventional processes like HIP.

J.R. Groza, Department of Mechanical, Aeronautical and Materials Engineering, University of California, Davis, California.

2. Principles of Pressure-Assisted Consolidation

To understand the principles of nonconventional consolidation, a general discussion of the pressure-assisted powder consolidation process is provided. Significant advances in the understanding of the mechanisms that contribute to pressure-assisted powder densification process have been made by Ashby and co-workers.[2-10] Although the pressure sintering mechanisms were mainly developed for the HIP process, the physics of the pressure-assisted sintering process remains essentially the same regardless of the pressure range. Extremely high pressures, though, as in shock wave consolidation, result in a different consolidation mechanism,[11] but this is outside of the scope of this article. The principles of pressure-assisted densification that will be presented basically follow the HIP process models, for which abundant literature is available.[2-10,12]

The sintering process may be divided mainly into two stages based on density values: the initial stage, or stage 1, with densities less than 90% of theoretical density, and the final stage, stage 2, with densities larger than 90%. In the initial stage, the particles are still recognizable and may be considered as spheres. For simplicity, they are considered to be of the same size. Bidimensional size distribution recently has been considered,[13] but this article is limited to the simple case of monosize particles. In the initial stage of densification, the necks (contact areas) are discrete, and the porosity is still interconnected. The densification process may be regarded as deter-

mined by the expansion of an initial sphere of radius R about its center to a new particle radius R' which is given by:[5]

$$R' = (D/D_0)^{1/3}R \quad [1]$$

where D is relative density, and D_0 the initial relative density (usually 64%). As spheres grow, the number, Z, of contact neighbors and the total contact area per particle, aZ (where a is the average contact area at a neck), increase. The normalized total contact area, a_t, defined as the total contact area on the surface of one particle normalized by the total area of the particle, was approximated by Helle et al.[6] as:

$$a_t = \frac{aZ}{4\pi R^2} = \frac{D(D - D_0)}{1 - D_0} \quad [2]$$

This contact area varies from zero at the initial packing density ($D = D_0$), when particles touch only at points, to unity at full density (as D approaches 1), when particles contact over entire surface area. In the initial stage, the particle deformation is confined to the contact regions. The contact pressure[6] depends on the total contact area on the surface of one particle, and the effective pressure, P_{eff}, on any particle contact during stage 1 is merely the external pressure, P, distributed over these contact areas at a current density D:

$$P_{eff} = \frac{P}{Da_t} = \frac{4\pi R^2}{aZD}P \quad [3]$$

Equation 3 neglects the pressure resulting from surface tension and entrapped gas effects, because they are insignificant compared to the external pressure. As will be shown later, this assumption is valid in those nonconventional compaction methods that involve removal of the entrapped gases. In the HIP process, however, the gas effects may be also ignored if an outgassing operation is performed prior to consolidation. Considering the average area of contact, a, as given by Helle et al:[6]

$$a = \frac{\pi(D - D_0)}{3(1 - D_0)}R^2 \quad [4]$$

with $Z = 12D$, as the number of contacts per particle, the effective pressure[6] may be obtained as:

$$P_{eff} = \frac{P(1 - D_0)}{D^2(D - D_0)} \quad [5]$$

The point contacts between particles when pressure is first applied (at $D = D_0$) results in infinitely high effective pressure values. As the contact area increases, the effective pressure falls and becomes equal to the applied pressure when full density is reached (D goes to 1).

In the final stage of densification, the solid is considered homogeneous, and the porosity is closed with spherical and equal size pores. If a good particle shape approximation is tetrakaidecahedral, then the pore radius is:[6]

$$r = R\left(\frac{1 - D}{6}\right)^{1/3} \quad [6]$$

As already shown, the effective pressure on particles may be equal to the applied pressure if the surface tension and pressure from entrapped gases are negligible.

2.1 *Mechanisms of Densification*

There are three main mechanisms that contribute to densification under pressure: plastic yielding, power-law creep, and diffusional densification. Although the latter mechanism exists in the pressureless sintering process and it is only enhanced by pressure application, the former two mechanisms are specific to pressure-assisted densification. The local rates of densification by plasticity, power-law creep, and diffusion are determined by the effective pressure at the particle contact regions. The total densification rate is the sum of all of these contributions, but for simplicity, each contribution will be presented separately.

2.1.1 *Plastic Yielding*

As shown above, when the external pressure, P, is applied, the effective pressure at the neck is very high because of the point contact area between particles. This high effective pressure may locally exceed the flow strength of the material and cause plastic yielding. This plastic yielding, in turn, increases the average contact area and causes the effective pressure to fall below the yield stress, σ_y. Yielding will occur during the initial densification stage provided that:[6]

$$P_{eff} \geq 3\,\sigma_y \quad [7]$$

If we use Eq 5 for P_{eff}, the external pressure that will just cause yielding, P_{lim}, is given by:

$$P_{lim} = 3D^2\frac{(D - D_0)}{(1 - D_0)}\sigma_y \approx 1.3\frac{(D^3 - D_0^3)}{(1 - D_0)}\sigma_y \quad [8]$$

Densification by plastic yielding is instantaneous in the initial stage, and the starting density, D_{yield}, may be obtained from Eq 8 as:

$$D_{yield} = \left(\frac{(1 - D_0)P}{1.3\sigma_y} + D_0^3\right)^{1/3} \quad [9]$$

The compact enters the final densification stage during plastic yielding only if pressure is high enough to cause yielding of the spherical shell surrounding each pore. The starting density given by yielding[6] in this final stage is:

$$D_{yield} = 1 - \exp\left(-\frac{3}{2}\frac{P}{\sigma_y}\right) \quad [10]$$

As will be shown later, some nonconventional consolidation processes may develop such high pressures that densification is accomplished solely by plastic yielding.

2.1.2 *Densification by Power-Law Creep*

When yielding stops, the contact area continues to increase by power-law creep. The densification rate by power-law creep during the initial stage is:[5,6]

$$\dot{D} = 3(D^2D_0)^{1/3}\left(\frac{D - D_0}{1 - D_0}\right)^{1/2}\left(\frac{\dot{\varepsilon}_0}{\sigma_0^n}\right)\left(\frac{P_{eff}}{3}\right)^n \quad [11]$$

where $\dot{\varepsilon}_0$, σ_0 and n are material creep parameters. The densification rate in the final stage is:[6]

$$\dot{D} = \frac{3}{2}\left(\frac{\dot{\varepsilon}_0}{\sigma_0^n}\right)\frac{D(1-D)}{\left[1-(1-D)^{1/n}\right]^n}\left(\frac{3}{2n}P\right)^n \quad [12]$$

Power-law creep is expected to have little contribution to densification in nonconventional high-pressure processes in which the time interval at high temperature is characteristically short.

2.1.3 *Densification by Diffusion*

Both grain boundary and lattice diffusion contribute to the matter transport from the contact zones to the surface of a sintering neck during the sintering process. Diffusion is accelerated by the externally applied pressure due to the increase in the surface tension driving force and to the shear stress components on the grain boundary between particles that promote atom displacement. Naumov et al. have shown that, in the plastic flow process under externally applied load, diffusional processes are extremely intensified due to a significant increase in lattice defect density.[14] Under these conditions, they showed that the density of lattice defects increases to the level of premelting temperatures. The densification rate in the initial stage combines the diffusion kinetics for one contact with the increase in coordination during densification. Starting with the detailed treatment of Wilkinson (shown in Ref 8) and lately simplified by Ashby,[8] this densification rate may be written as:

$$\dot{D} = A\frac{P_{\text{eff}}\Omega}{R^3}\left[\frac{D_v}{kT}R\,(D-D_0) + \frac{\delta D_b}{kT}\right] \quad [13]$$

where $A = c_1\,(1-D_0)^2/(D-D_0)^2$; c_1 is a numerical constant; Ω is the volume of the diffusing atom or molecule; D_v is the lattice diffusion coefficient; δD_b is the boundary diffusion coefficient times its thickness; and kT has the standard meaning. Because many small contacts densify faster than a few large ones, the contact area considered is not aZ, but the average area of a single contact. Therefore, the rate of the diffusional mechanism is strongly dependent on particle size, R. This is in contrast to the power-law creep densification rate, which is independent of R (Eq 11 and 12). The diffusional contribution to the densification rate in the final stage is given by the following equation:[8]

$$\dot{D} = B\frac{P\Omega}{R^3}\left[\frac{D_v}{kT}R(1-D)^{1/3} + \frac{\delta DB}{kT}\right] \quad [14]$$

where $B = c_2\,(1-D)^{1/2}$ and c_2 is a numerical constant. The predominant process varies with temperature. At high temperatures, lattice diffusion controls the rate; at lower temperatures, grain boundary diffusion takes over. The intensification of diffusional processes due to plastic flow is expected to occur in the final stage of densification when contact surface areas become important.

2.1.4 *Pressure Sintering Maps*

The total densification rate is the sum of all contributions that were defined above. However, it has been found that one contribution is almost always dominant in certain conditions, and regions for these rate-controlling mechanisms may be defined as functions of pressure and temperature. The results from each densification mechanism are assembled into densification maps that show the density as a function of pressure, temperature, and/or time. These maps identify the dominant mechanism and predict densification rates and times as functions of external variables. Such maps are available for a variety of materials.[5-7,13,15] A computer program developed by Ashby is now available for HIP map generation.[10] The distinctive use of these maps in the present article is to identify the mechanisms that control the rate of densification for various consolidation methods. In this way, more insight may be gained on the specific mechanisms of each consolidation method and the change in the densification rate with process parameters.

3. Nonconventional Compaction Techniques

As already described, applied pressure enhances the powder compaction process by rearranging the particles, inducing plasticity and creep, and augmenting the diffusional processes. Numerous such pressure-assisted consolidation techniques have been developed, and they are listed in Table 1 according to applied pressure range. For comparison, explosive consolidation at very high pressures for extremely short times and hot isostatic pressing (HIP) with low pressures but applied for substantially long times are shown. Cold sintering uses high pressures in short time, but full densities are achieved by subsequent warm sintering.[16,17] A similar method of cold sintering is "pressure + torsion" at room temperature up to very high deformation levels developed by Korznikov et al.[18] The consolidation methods of current interest are those combining medium to high pressures and short consolidation times (on the order of minutes) at high temperatures. These include Ceracon,

Table 1 Comparison of pressure-assisted densification process

Process	Pressure, GPa	Duration, s	Directionality
Hot pressing	0.01-0.03	10^3-10^4	Uniaxial
Hot isostatic pressing (HIP)	0.10-0.30	10^3-10^4	Isostatic
Hot extrusion	0.10-1.00	10^2-10^4	Complex
Rapid omnidirectional consolidation (ROC)	0.10-1.00	10-10^2	Quasi-isostatic
Ceracon	0.10-2.00	10-10^3	Quasi-isostatic
Plasma-activated sintering (PAS)	0.01-0.1	10-10^2	Uniaxial
Cold pressing	3-4.5	~10	Uniaxial
Explosive consolidation	10.00-100.00	~10^{-6}	Complex

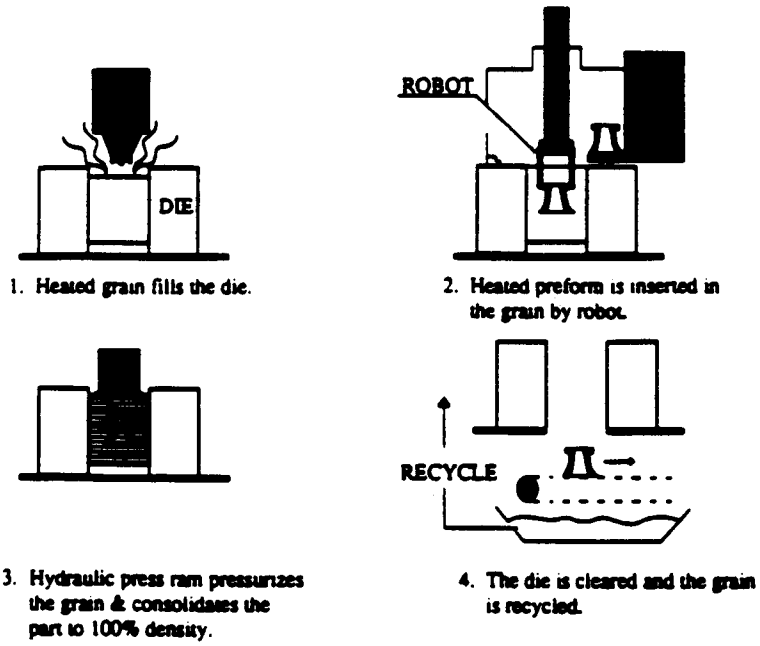

Fig. 1 Schematic of the Ceracon consolidation process.[22]

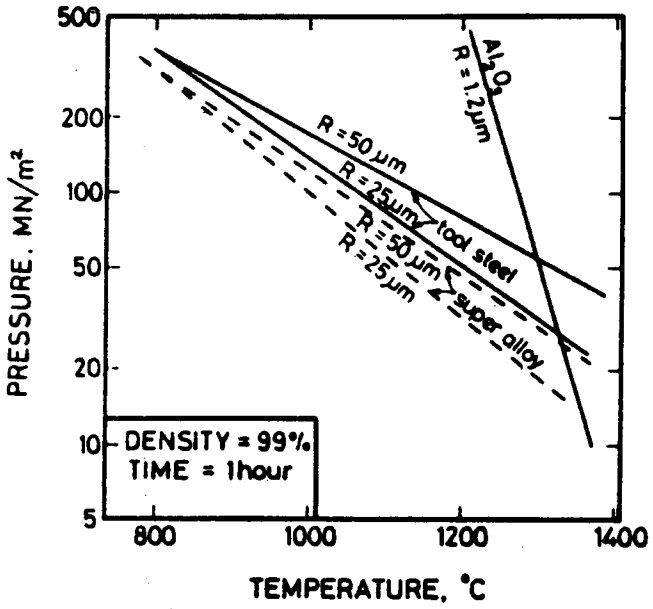

Fig. 2 Trade-off between the pressure and temperature needed to achieve 99% density in 1 h for various materials.[5]

rapid omnidirectional consolidation (ROC), and plasma-activated sintering (PAS). The first two processes are accomplished at higher pressures than HIP such that trade-offs between pressure and temperature are possible to preserve metastability in the final compact. Plasma-activated sintering is a recently developed consolidation process that involves a plasma discharge to activate particle surfaces and thus enhance particle sinterability and reduce the high-temperature exposure.

The directionality of forces imposed (shear versus pressure components) in various consolidation techniques is a useful criterion for their comparison (Table 1). This directionality implies the ratio of shear versus normal stress components. An isostatic pressure is comprised mainly of normal compression stresses. This is the case in HIP, although some deviatoric, nonhydrostatic stresses may appear due to nonuniformities in the HIP system.[8,9,19,20]These stresses are nevertheless small[9] and will be neglected in this comparison. The quasi-isostatic pressure application such as that used in Ceracon or ROC processes inherently involves a certain, controllable amount of nonhydrostatic (shear) components. The shear component becomes important in the consolidation of those systems in which the oxide layers on powder particles are particularly adherent and stable (e.g., aluminum oxide). The shear stress ensures relative motion between the opposite sides of collapsing pores, which results in mechanical fracturing of surface oxides. Consequently, new clean areas are exposed, and an efficient bonding of powder particle surfaces may be developed. Evidently, the extrusion and forging processes will have the highest shear stresses and, therefore, the highest densification capabilities for systems with stable oxides.

3.1 *High-Pressure Quasi-Isostatic Consolidation Processes*

The quasi-isostatic Ceracon process is schematically depicted in Fig. 1.[21-23] This process uses high-temperature-resistant granules as the pressure-transmitting medium in place of fluids used in hot isostatic pressing. Preforms of the material to be densified are immersed in the granular medium, and uniaxial pressure is applied to the bed of particles. When the axial load is applied to a granular medium, the particles flow easily around the preform to distribute applied pressure essentially

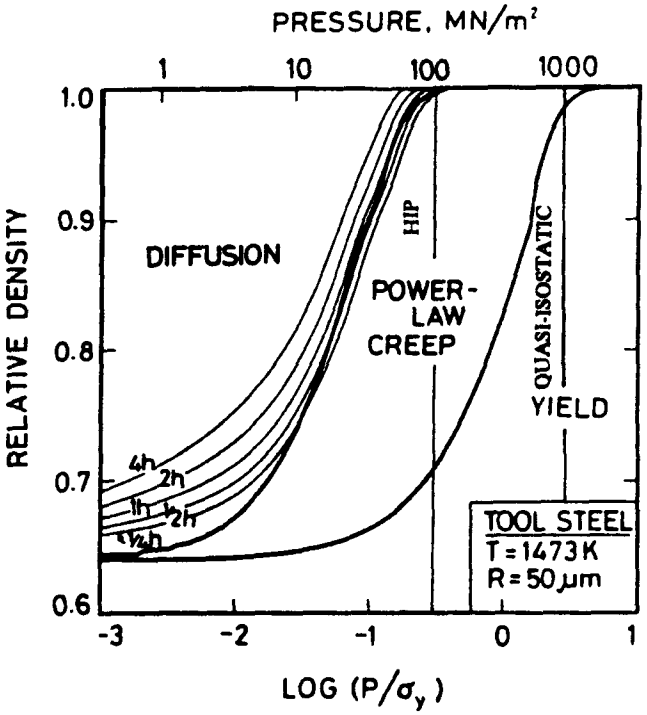

Fig. 3 HIP and quasi-isostatic densification conditions for tool steel with a particle size of 50 μm at 1473 K.

in a quasi-isostatical manner. The Ceracon process may be controlled to induce various ratios of shear to normal pressure components by die design and selection of pressurizing medium type. The rapid omnidirectional compression (ROC) process pertains to the quasi-isostatic consolidation process category as well. The main differentiation of ROC from the Ceracon process is in the nature of the pressure-transmitting medium. In the ROC process, a "fluid" (a highly deformable material at working temperature such as metals or glasses) die applies a near-isostatic pressure field to the encased powder.[24]

As already shown, these nonconventional processes combine higher pressures and shorter times than HIP. They rely on the well-known trade-off between pressure and temperature to achieve the same density. For illustration, such a pressure/temperature map is shown in Fig. 2, in which the pressure/temperature combinations to obtain the same relative density of 99% in 1 h are shown for different materials.[5] For metallic materials, a pressure increase of one order of magnitude results in a decrease of the consolidation temperature from about 0.8 T_m to 0.5 to 0.6 T_m. This drop in temperature results in a decrease in the rate of grain growth by roughly five to nine orders of magnitude if Arrhenius behavior is considered with an activation energy of 300 kJ/mol.[25] Consequently, the suppression of grain growth that is critical to ultrafine materials is achievable in high-pressure consolidation processes by reducing processing temperatures. Finally, the short-time pressure application that is characteristic of high-pressure processes is also instrumental for fine-grain structure retention.

To evaluate the quasi-isostatic processes versus HIP, a comparison of consolidation conditions is shown in Fig. 3, which describes the densification of tool steels taken from the work of Arzt et al.[5] This comparison is only informative, but depicts fairly accurately the differences between the dominant mechanisms involved in HIP versus quasi-isostatic consolidation methods. For the usual HIP conditions at a pressure of about 100 MPa, the map shows that plastic yield contributes to densification in the initial stage. This is the stage when only point contact areas between particles exist. This pressure value is not sufficient to exceed the material yield stress when larger contact areas develop. Therefore, further densification is achieved by power-law creep, which, according to Fig. 3, is the principal mechanism. Finally, full density is obtained by diffusion-controlled densification. At high pressures, for instance at 1 GPa, the plastic yield becomes the predominant densification process (the quasi-isostatic line in Fig. 3). The final stages of densification are accomplished by power-law creep. At very high pressures, above 2 GPa for tool steel, full densification may be achieved exclusively by plastic yielding, and densification is almost instantaneous. The above example clearly shows that high-pressure application significantly shortens consolidation times. Furthermore, high pressures may also be substituted for high temperatures. As already discussed, the trade-offs between higher pressures and low temperatures are shown in Fig. 2 (the line labeled "tool steel"); a fourfold increase in pressure, i.e., from 100 to 400 MPa, results in a decrease in consolidation temperature by about 380 K at the same sintering duration. As shown above, this level of pressure and higher values are achievable in the quasi-isostatic regimes.

As expected, the quasi-isostatic processes—Ceracon and ROC—provide similar consolidation conditions. For example, the difficult-to-sinter titanium aluminides powders can be consolidated by both Ceracon and ROC processes.[22-24] Titanium aluminide powders are difficult to deform due to their inherent brittleness as intermetallic compounds and stable aluminum oxide layer on the particle surface. Ceracon consolidation was applied to rapidly solidified TiAl powders and resulted in fully dense material at 1473 K under a pressure of 1.24 GPa that was applied for 45 s.[22,23] The details of the powders and compaction process are given elsewhere.[23] The full density achieved for TiAl compacts is an indication that the Ceracon process may provide enough shearing stress to cause oxide rupturing and subsequent welding of freshly exposed surfaces. As expected, at this high pressure level, the Ceracon consolidation process is mainly achieved by plastic yielding, as shown in Fig. 4. In this figure, the Ceracon line lies very closely to the boundary between time-dependent (power-law creep) and time-independent (plastic yielding) mechanisms. The longer dwell time than that typical to the Ceracon process may be an indication that time-dependent processes may also play a role in TiAl densification, in agreement with the pressure sintering diagram shown in Fig. 4. However, an alternate explanation may be considered for this longer dwell time, as recently pointed out for the HIP process.[19] This explanation takes into account the time necessary for TiAl material to reach the high test pressure. This delay may be of importance in the Ceracon process, in which the stress is applied by an intermediate granular pressurizing medium. At the same time, there may be a degree of uncertainty in the position of the densification boundaries in Fig. 4. Further work is necessary to define the possible contribu-

tions to the unusual long time of the Ceracon consolidation of TiAl intermetallic.

These results on TiAl processed by Ceracon consolidation compare favorably with conventional consolidation conditions. For instance, only a high deformation ratio (16:1) and a high temperature, 1700 K, resulted in successful consolidation of TiAl by extrusion.[26] Similarly, hot isostatic pressing had to be followed by hot extrusion to obtain a homogenous structure in bulk TiAl material.[27]

Unfortunately, there are no data available for TiAl ROC consolidation. However, ROC was applied to other aluminides (Ti_3Al) that were consolidated while retaining the extremely fine grain size.[24,28] The mechanical properties of ROC-processed materials are comparable or better than those of wrought materials.[24]

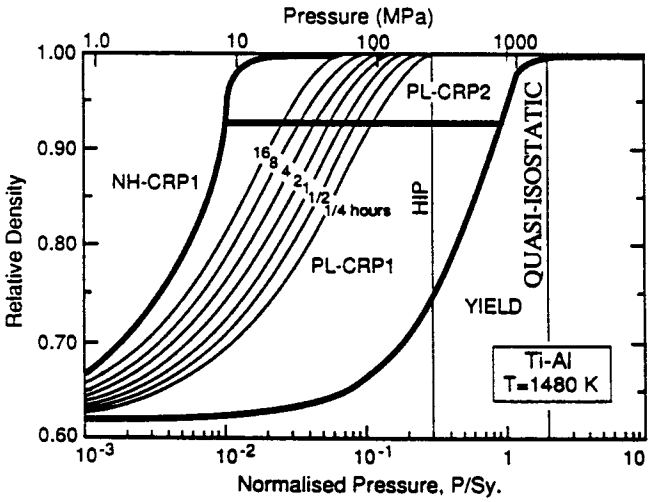

Fig. 4 Densification diagram for TiAl powders with an initial packing density of 62% at 1480 K.[23] NH-CRP 1—Nabarro-Herring creep in stage 1 of densification. PL-CRP 1 and PL-CRP 2—power law creep in stage 1 and 2 of densification, respectively.

3.2 *Plasma-Activated Sintering Process*

The PAS process is schematically depicted in Fig. 5. In this process, plasma is first generated by instantaneous pulsed electric power application to activate the particle surface (control switch at right). The powder particles are subsequently resistance heated (control switch at left) as uniaxial pressure is simultaneously applied to the sample in the sintering mold. The pressure application time is short, but causes sufficient plastic yielding and material flow for rapid consolidation. No studies exist to explain the plasma-activated sintering process. However, some similarities with electrodischarge compaction[29-31] and resistance sintering[32-34] may be established. The experimental data on PAS consolidated powders are also extremely limited.[35,36] Therefore, at this time, only deductions on densification mechanisms are possible. It is assumed that the accelerated PAS densification may be attributed to a combination of electrical discharge, resistance heating, and pressure application effects. In electrical discharge, energy emission is concentrated at particle contacts that attain high temperatures.[29] These concentrated heat effects at particle surfaces may cause surface melting and oxide breakdown, similar to surface effects in electrodischarge machining. In other applications of pulse electrical current such as for thermosynthesis of chemical compounds, an enhanced reaction was also observed.[37] This intensification of the reaction was attributed to the breakage of the oxide films on the surface of reacting powders. Based on the above information, the same plasma effect may take place in the PAS process. The initial electrical pulse application will break up the oxide films and expose new clean areas for subsequent welding. This process may be partially regarded as an activation of particle surface or an *in situ* cleaning action of powder particles by the removal of surface oxides and entrapped gases. This surface cleaning from oxides is important for two main reasons. First, the newly cleaned and activated surfaces contribute to enhanced diffusion and welding

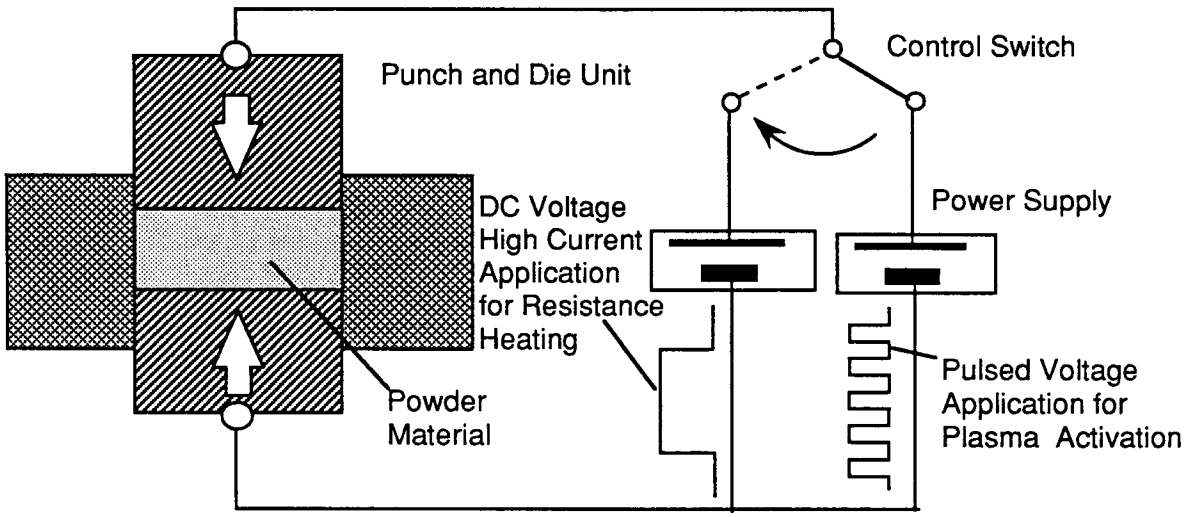

Fig. 5 Schematic of the PAS consolidation process.

during subsequent densification. Second, for many materials, the oxide film on the particle boundaries in consolidated material may have deleterious effects on their physical and mechanical properties. This *in situ* cleaning action becomes more important for oxygen-sensitive powders for which protection from oxygen contamination in early stages of powder preparation is practically impossible. The next step in PAS consolidation is the resistance heating. Generally, resistance heating is known to cause full densification by a liquid sintering mechanism.[32] Local surface melting occurs due to higher electrical resistance of surface oxides. In the plasma-activated sintering process, however, the prior plasma activation step removes surface oxides and melting related to higher electrical resistance of surface films is less likely to occur. However, as already shown, surface melting might be caused by electrical discharge action. Finally, mechanical pressure is applied on heated particles. The addition of external pressure facilitates full compaction during both liquid sintering and solid-state densification. This conclusion is supported by significantly shorter consolidation times in PAS than in HIP (Table 1), whereas the level of mechanical pressure is comparable. These shorter times are a good indication that solid-state time-dependent mechanisms (such as creep in HIP) do not significantly contribute to densification. Instead, accelerated atomic motion such as liquid diffusion or enhanced surface diffusion at the activated particle surface leads to full densification. Unfortunately, no experimental evidence is available to date to substantiate this statement. The current preliminary microstructural observation on PAS-consolidated AlN did not reveal any secondary grain boundary phases within the limits of resolution of the TEM.[35] Such grain boundary phases might have indicated a liquid sintering process. Characterization studies on various PAS-consolidated materials, with the aim of evaluating the liquid presence during densification, are in progress. Even for simple resistance sintering processes, the microstructural characteristics shown to support the liquid formation are not convincing. For example, Liu and Kao reported consolidation of titanium by resistance sintering.[32] The optical microstructure of sintered titanium contains a "secondary" α that, according to them, has formed from a liquid phase. Unless our measurements are in serious error, the secondary α spacing is significantly different from initial powder size. If melting occurs at particle surfaces, one can expect that secondary α will have the same distribution as the initial particles.

In conclusion, due to the combination of mechanical pressure, electrical field application, and plasma activation, the PAS sintering process is capable of consolidating difficult-to-sinter, highly oxygen-sensitive materials with minimum microstructural changes. For example, densities in excess of 99% were obtained in covalent AlN ceramics at 2000 K under applied pressures of 50 MPa for 5 min.[35] The initial submicron grain size has been retained. This retention of grain size may be attributed to a significantly shorter high-temperature exposure of the powder particles. For comparison, in conventional sintering conditions for AlN powders, temperatures are at least 2100 K for several hours.[38]

Intermetallic compound synthesis and powder densification have been simultaneously achieved by PAS consolidation of nanocrystalline Nb-Al powders obtained by mechanical alloying.[39] Full-density compacts of these highly oxygen-sensitive powders were obtained, again confirming the high densification ability of the plasma-activated sintering process.

4. Conclusions

The densification theory and applications of nonconventional consolidation methods—Ceracon, rapid omnidirectional consolidation, and plasma-activated sintering—were presented. The quasi-isostatic nonconventional consolidation methods consist of usually high-pressure application for short times at high temperatures. The dominant densification mechanism is plastic yielding. The pressure application not only produces strong plastic flow, but also significantly enhances the diffusional processes.

Special densification behavior occurs in the presence of a plasma-activated environment. The activation of particle surface and cleaning power of the plasma discharge confer unique densification ability for difficult-to-sinter materials such as covalent ceramics or highly oxygen-sensitive powders. High densities compacts of covalent AlN ceramic and simultaneous densification and synthesis of the Nb_3Al compound were obtained by plasma-activated sintering.

Acknowledgments

The author is grateful to J.C. Gibeling for critically reading the manuscript and to Ceracon Inc., Sacramento, for providing technical information.

References

1. Nanostructured Materials Workshop, NIST, Gaithersburg, May 14-15, 1992
2. M.F. Ashby, *Acta Metall.*, Vol 22, 1974, p 275
3. F.G. Swinkels and M.F. Ashby, *Acta Metall.*, Vol 29, 1981, p 259
4. F.B. Swinkels, D.S. Wilkinson, E. Arzt, and M.F. Ashby, *Acta Metall.*, Vol 31, 1983, p 1829
5. E. Arzt, M.F. Ashby, and K.E. Easterling, *Metall. Trans. A*, Vol 14, 1983, p 211
6. A.S. Helle, K.E. Easterling, and M.F. Ashby, *Acta Metall.*, Vol 33, 1985, p 2163
7. H.J. Frost and M.F. Ashby, The Plasticity and Creep of Metals and Ceramics, in *Deformation-Mechanism Maps*, Pergamon Press, 1982, p 1
8. M.F. Ashby, "Powders Compaction under Non-Hydrostatic Stress States. An Initial Survey," presented at the meeting for Powder Compaction Modeling, BDM Co., Arlington, VA, 1990
9. H.N.G. Wadley, R.J.Schaefer, A.H. Kahn, M.F. Ashby, R.B. Clough, Y. Geffen, and J.J. Wlassich, *Acta Metall. Mater.*, Vol 39, 1992, p 986
10. M.F. Ashby, *Operating Manual for HIP 487*, Version HIP 6.0, Cambridge University, 1987, 1990
11. R.B. Schwarz, P. Kasiraj, T. Vreeland, Jr., and T.J. Ahrens, *Acta Metall.*, Vol 32, 1984, p 1243
12. R.M. McMeeking and L.T. Kuhn, *Acta Metall. Mater.*, Vol 40, 1992, p 961
13. R.N. Wright, R.L. Williamson, and J.R. Knibloe, *Powder Metall.*, Vol 33, 1990, p 253
14. I.I. Naumov, G.A. Ol'khovik, and V.E. Panin, *Izv. Akad. Nauk SSSR, Metally.*, No. 1, 1990, p 152

15. N. Ramakrishnan and V.S. Arunachalam in *Powder Metallurgy—Recent Advances*, V.S. Arunachalam and O.V. Roman, Ed., Aspect Publ., London, 1990, p 66
16. E.Y. Gutmanas, in *New Materials by Mechanical Alloying Techniques*, E. Arzt and L. Schultz, Ed., DGM Informationsgesellschaft, Oberusel, 1989, p 129
17. E.Y. Gutmanas and A. Lawley, in *1990 Advances in Powder Metallurgy*, E.R. Andreotti and P.J. McGeehan, Ed., MPIF, APMI, Princeton, 1990, p 1
18. A.V. Korznikov, I.M. Safarov, D.V. Laptionok, and R.Z. Valiev, *Acta Metall. Mater.*, Vol 39, 1991, p 3192
19. W.-B. Li, K.E. Easterling, and M. F. Ashby, *Met. Trans.*, Vol 22A, 1991, p 1071
20. L.T. Kuhn and R.M. McMeeking, *Constitutive Laws for Powder Compaction under Non-Hydrostatic Stress States*, University of California, Santa Barbara, 1991
21. R.L. Anderson and J.R. Groza, *Met. Powder Rep.*, Vol 43, 1988, p 678
22. R.V. Raman, *Adv. Mater. Process.*, Vol 137, 1990, p 109
23. C.G. Levi, R. Mehrabian, B. Oslin, R.L. Anderson, and S.M.L. Sastry, *J. Mater. Shaping Technol.*, Vol 6, 1988, p 125
24. C.A. Kelto and E.E. Timm, *Ann. Rev. Mater. Sci.*, Vol 19, 1989, p 527
25. J.G. Byrne, *Recovery, Recrystallization and Grain Growth*, Macmillan, London, 1965, p 139
26. R.E. Schafrik, *Metall. Trans. B*, Vol 7B, 1976, p 713
27. S-C. Huang and E.L. Hall, *Metall. Trans. A*, Vol 22A, 1991, p 2619
28. W. J. Porter, N.R. Osborne, D. Eylon, and J.P. Clifford, in *1990 Advances in Powder Metallurgy*, E.R. Andreotti and P. J. McGeehan, Ed., MPIF, APMI, Princeton, 1990, p 243
29. V.N. Bazanov, S.A. Balankin, Je.G. Grigoriev, V.V. Gunichev, S.V. Novikov, and V.A. Yartsev, in *PM'90, PM into the 1990's, International Conference on Powder Metallurgy*, The Institute of Metals, London, 1990, p 270
30. D.K. Kim and K. Okazaki, in *1991 P/M in Aerospace and Defense Technologies*, Tampa, 4-6 March 1991, MPIF, AMPI, Princeton, 1991, p 365
31. P.A. Vityaz, V.M. Kaptevich, K.E. Belyavin, and A.A. Gurevich, in *PM'90, PM into the 1990's, International Conference on Powder Metallurgy*, The Institute of Metals, London, 1990, p 271
32. C.H. Liu and P.W. Kao, *Scr. Metall. Mater.*, Vol 24, 1990, p 2279
33. S.J. Hong and P.W. Kao, *Mater. Sci. Eng.*, Vol A119, 1989, p 153
34. S.J. Hong and P.W. Kao, *Mater. Sci. Eng.*, Vol A148, 1989, p 189
35. J.R. Groza, S. Risbud, and K. Yamazaki, *J. Mater. Res.*, Vol 7, 1992, p 2643
36. S. Nagata, Y. Takahashi, M. Yorizumi, and K. Aso, "Fine Grained Mn-Zn Ferrite Produced by Plasma Sintering Method (PAS)," presented at the 6th Int. Conf. Ferrite, Kyoto, Japan, 1992
37. S.A. Balankin, V.S. Sokolov, and A.O. Troitzkiy, in *PM'90, PM into the 1990's, International Conference on Powder Metallurgy*, The Institute of Metals, London, 1990, p 37
38. I. Teusel and C. Russel, *J. Mater. Sci. Lett.*, Vol 11, 1992, p 205
39. M. Tracy and J. R. Groza, Nanophase Structure in Nb-Rich Nb_3Al Alloy by Mechanical Alloying, *NanoStructured Materials*, Vol 1, 1992, p 369